NASA Technical Memorandum 83316

Long-Term Predictive Capability of Erosion Models

P. Veerabhadra Rao and Donald H. Buckley
Lewis Research Center
Cleveland, Ohio

Prepared for the
Seventh Conference on Fluid Machinery
sponsored by the Scientific Society of Mechanical Engineers
Budapest, Hungary, September 13-16, 1983

NASA

LONG-TERM PREDICTIVE CAPABILITY OF EROSION MODELS

P. Veerabhadra Rao and Donald H. Buckley

National Aeronautics and Space Administration
Lewis Research Center
Cleveland, Ohio 44135

ABSTRACT

This paper reports a brief overview of long-term cavitation and liquid impingement erosion and modeling methods proposed by different investigators, incliding the curve-fit approach recently suggested from this laboratory. A table is prepared to highlight the number of variables necessary for each model in order to compute the erosion-versus-time curves. A power law relation based on the average erosion rate is suggested which may solve several modeling problems.

E-1543

INTRODUCTION

Long-term prediction of erosion due to cavitation and liquid impingement has become very important in view of severe erosion problems associated with hydraulic turbines and pumps due to cavitation, with aircraft surfaces due to rain drops, and with steam turbine blades due to impingement of condensed droplets. Extended periods of reliable operation in all situations reemphasized the necessity for erosion-free performance or the alleviation of erosion. In most cases complete elimination of erosion is not possible. Hence, it is necessary to establish the total erosion of a material for prolonged operation so that the particular component may be changed, or so that highly resistant materials may be used to increase component life.

Although Honegger (ref. 1) was the first investigator to notice the effect of exposure time on erosion rate, Fyall et al. (ref. 2) in 1957, Hobbs (ref. 3) in 1962, and Thiruvengadam (refs. 4 and 5) in the early 1960's clearly observed the influence of time on instantaneous erosion rate.[1] Investigations by Thiruvengadam and Presier (ref. 6), Plesset and Devine (ref. 7), Heymann (ref. 8), and Tichler and de Gee (ref. 9) have become classic studies. There have been, however, several discrepancies in the agreement of the type of erosion-rate-versus-time curves.[2] Using shapes of curves obtained earlier, many models and formulations have been presented by different investigators for the long-term prediction of cavitation and liquid impingement erosion (refs. 8 to 14). The details of the models are reviewed and presented in reference 15. Table 1 presents models proposed and the number of variables necessary to predict erosion using these models (refs. 14 and 15).

---

[1]Instantaneous erosion rate equals slope of local tangent on erosion-versus-time curves

[2]Curves reported in reference 6 contain incubation, acceleration, deceleration, and steady-state zones; in reference 7, incubation, acceleration, steady-state, and deceleration zones; in reference 8, peak erosion and deceleration zones or acceleration zone and several cycles of peaks of erosion rate; and in reference 9, incubation, acceleration, first steady-state, deceleration and second steady-state periods.

SYMBOLS

A	constant or coefficient
a_1	parameter representing inner friction of material during plastic deformation
a_2	a scale of cavitation strength of material
B	exponential constant (fig. 1) or coefficient (eq. (4))
C	coefficient (eq. (7))
$\dot{e}$	erosion rate at any time τ
$\dot{e}_{max}$	maximum or peak erosion rate
T	I_e/I_{max}
I_e	intensity of erosion at any time τ
I_{max}	maximum intensity of erosion
$\overline{K}$	$(dn/d\tau)_{\tau=1}$
max	maximum
N_e	generalized nondimensional erosion resistance parameter defined as the ratio of the measured erosion rate of the material to the measured erosion rate of the material to be evaluated
n	attenuation exponent (fig. 2) or exponent (eqs. (1) and (2))
n_ω	number of craters per unit area in final steady-state period
P	exponent
R	averaged erosion rate up to a cumulative material loss Y
R_c	resistance against cavitation erosion under the hydrodynamic conditions as in magnetostriction oscillator
R_T	averaged erosion rate at tangent point corresponding to a cumulative material loss Y_T
R_ω	resistance against cavitation erosion during the second steady-state condition
r	mean depth of erosion at any time t
r_b	mean depth of erosion at which the effect of crater formation becomes manifest
t	exposure time to cavitation (figs. 2, 4, and 5) or incubation period (fig. 3)
t_m	time corresponding to the maximum intensity of erosion
t_o	incubation period (fig. 4)
t_Y	time required to reach a mean erosion depth of Y (sec)

U_a	volume of liquid impinging per unit area per unit time (μm/sec)
v	cavitation damage rate = $\Delta m/\Delta t$
V	cumulation volume loss, mm^3
V_o	normal component of impact velocity (m/sec)
v_s	steady-state cavitation damage rate
Y	cumulative mean depth of erosion or material loss at any instant
Y_T	cumulative mean depth of erosion or material loss at tangent point
α	Weibull shape parameter (fig. 2) or parameter representing inner friction of material during plastic deformation = $a_1/2$ (fig. 5).
β	parameter representing square root of a scale of cavitation strength of material = $\sqrt{a_2}$
Δm	cavitation damage of a material during time Δt
Δt	time increment
δ	parameter expressing cavitation properties of the material = α/β
ϵ_a	normalized average erosion rate with respect to peak erosion rate
η	efficiency of erosion at any time t = 1 - exp $(-\tau^\alpha)$
$\overline{\eta}$	η/η_{max}
η_{max}	efficiency of erosion corresponding to the peak or maximum intensity I_{max}
Θ	limiting value of δ
κ	a proportionality constant symbolizing the increase in mean depth of erosion ($r \geq r_b$) which would be necessary to form n^∞ craters
ν	relative cavitation damage = $\Delta m/(v_s \Delta t) = v/v_s$
ξ	log t
τ	t/t_m (in Thiruvengadam's theory of erosion, fig. 2) or exposure time (according to Hoff and Langbein equation, fig. 3) or relative cavitation time (fig. 5) = βt
ψ_∞	ratio between the rate of erosion in the final steady-state period and the rate of erosion in the first steady-state period

LONG-TERM PREDICTION MODELS

Equations or models for the prediction of erosion rate with respect to time have been proposed by Heymann (refs 8 and 12), Tichler and de Gee (ref. 9), Thiruvendagam (ref. 10), Hoff and Langbein (ref. 11), Noskievic (ref. 13), Engel (ref. 16), and Perelman and Denisov (ref. 17). McGuiness and Thiruvengadam (ref. 18) have studied the influence of corrosion on erosion in their modeling efforts. Others (refs. 19 and 20) have presented nomograms and

graphs. A brief description of the important contributions of these models is outlined below in order to explain the current status of erosion-rate-versus-time predictions for long-term exposures.

Heymann's Models

Elementary model. - Heymann (ref. 8) developed an elementary statistical erosion-rate-versus-time model for liquid impingement and cavitation erosion conditions of different materials wherein fatigue is the predominant failure mechanism. The model requires four parameters to obtain instantaneous erosion-rate-versus-time curves (table I). The fit of experimental data in certain real situations is very convincing with the use of normal distributions truncated and normalized over a finite time span.

Elaborate model. - Heymann's elaborated model (ref. 8) permits the specification of a different distribution function for each level below the original surface and of two different functions for the original surface. In this model the log-normal distribution is adopted. The inclusion of the median lifetime for the unaffected surface has significantly improved the predictions.

Curve-fit approach. - Heymann (ref. 12) suggested a simple curve-fit approach using tangent (cumulative average) rate of erosion[3] and tangent mean cumulative depth of erosion (volume loss) to predict the erosion rate which follows the peak erosion rate (fig. 1). Equations suggested for the calculation of normalized average erosion rate (R/R_T) and for time (t_v) to reach a mean erosion rate require three and four parameters, respectively, to compute the erosion-versus-time history (table I). For particular liquid impingement and cavitation erosion data sets, this approach appeared promising (ref. 12).

Thiruvengadam's Nomogram and Theory of Erosion

Strain energy. - Using a strain energy theory,[4] a nomogram was developed based on cavitation erosion data (refs. 19 and 21). This nomogram has been used by design engineers to predict life of materials with a knowledge of erosion intensity and strain energy. Unfortunately, strain energy is a good predictor only for highly ductile materials.

Concept of erosion strength and theory of erosion. - In view of the limitations of strain energy, Thiruvengadam later developed the concept of erosion strength[5]. Using this concept a theory of erosion (ref. 10) was developed

---

[3]Cumulative average erosion rate equals slope of line joining origin and point of consideration on erosion-versus-time curve.

[4]The area of a stress-strain curve is a measure of this energy per unit volume.

[5]The energy-absorbing capacity of the material per unit volume under the action of erosive forces or the ratio of energy absorbed by the material eroded to the volume of material eroded.

to predict nonlinear effects of time on erosion rate, to quantitatively arrive at meaningful correlations in the laboratory, and to extrapolate to field prototypes. Figure 2 present theoretical prediction curves of relative intensity (or relative erosion rate) versus relative time for an attenuation exponent n = 2. The final equation used is also presented in figure 2. This theory needs four parameters to compute the erosion-rate-versus-time curve (table I). Long-term predictive efforts using the theory of erosion (ref. 10) were also attempted by Thiruvengadam (ref. 22). Thiruvengadam also modified his nomogram using the concept of erosion strength instead of strain energy (ref. 23). For design engineers, this nomogram may possibly be useful for the rough estimation of erosion rate under cavitation and liquid impingement erosion conditions.

Hoff and Langbein Equation

A simple exponential equation was proposed by Hoff and Langbein (ref. 11) incorporating the heterogeneous characteristics of impingement drops based on impact statistics. The proposed equation (fig. 3) requires only two parameters in order to compute the erosion rate as a function of time (table I). It should be noted, however, that by introducing a Poisson distribution into the method proposed by Heymann (ref. 8) or by introducing a distribution function into the original method proposed by Hoff and Langbein (ref. 11), the two methods are quite similar.

Tichler and de Gee Model

Tichler and de Gee (ref. 9), on the basis of the observation of two steady-state periods, have formulated an equation to predict the mean depth of erosion as a function of time. It was assumed that the erosion rate is relatively high and the surface is attacked uniformly during the first steady-state period. The surface is saturated with deep isolated craters and the erosion rate is relatively low during the second steady-state period. The final equation suggested for attenuation and the second steady-state period and definition of terms used are presented in figure 4. The equation needs five parameters to define the mean depth of erosion-rate-versus-time curve (table I). A graphical method to determine these parameters was presented by the investigators.

Noskievic Formulation

Noskievic (ref. 13) formulated a mathematical relaxation model for the dynamics of caviation damage of materials using a differential equation applied to forced oscillations with damping. This cavitation erosion model requires three parameters for the prediction of an erosion-versus-time curve (table I). Charts are presented for the use of this method (fig. 5), which simplifies the hurdle of going through lengthy equations and calculations. The experimental curve of relative cavitation damage (υ) versus log cavitation exposure time (log t) has to be compared with curves in figure 5 by shifting in the direction of the log t axis until a curve of approximate match is found. This enables one to read out δ and τ, which results in a β value.

Curve-Fit Approach

Data for a large number of materials tested in both a rotating disk device and a magnetostriction oscillator have been analyzed in a manner that presents normalized cumulative average erosion rate versus normalized time

which brings the results to a universal curve fit (ref. 14). With a knowledge of four parameters (table I), it may be possible to correlate erosion data between the laboratory model and field devices. The agreement of the data analyzed from two previous investigations with entirely different experimental conditions not only showed similarities between cavitation and liquid-impingment erosion, but also reinforced the possibility of the unified nature of erosion. Correction factors for the incubation period and intensity of erosion are suggested.

DISCUSSION

Figure 6 presents normalized-average-erosion-rate-versus-normalized-time curves for stainless steel tested in a rotating disk device (ref. 14). The data are normalized with respect to peak erosion rate and the time corresponding to this peak. Models proposed by Thiruvengadam (ref. 10), and Heymann (ref. 12), and a curve-fit normalization technique by Rao and Young (ref. 14), have also been presented on the curve. The methods proposed in references 10 and 12 fit the data following the peak erosion rate. It is noted, however, that normalized time from 0 to 1 cannot be represented by any of the equations presented earlier, except the curve-fit approach developed at this laboratory (ref. 14). The methods proposed by Tichler and de Gee (ref. 9) and Noskievic (ref. 13) have not been used, as the data considered for the analysis was not exposed too long and their plots represent a different dependent parameter. For individual materials, good results can be obtained at a single experimental condition with these two methods. It must be indicated, however, that many calculations are needed with these two methods.

To check the general validity of the models and graphical approaches presented earlier, data reported for cavitation erosion (refs. 24 and 25) and liquid impingement (ref. 26 and 27) were analyzed. A typical set of plots is presented in figures 7 to 9 as normalized average erosion rate versus normalized time. It is evident that a material tested at a variety of conditions cannot be represented by a single method proposed earlier for long-term predictions. When individual groups of materials are considered, as in figure 9, the methods proposed by Thiruvengadam (ref. 10) and Heymann (ref. 12) are good. To show the involvement of calculations with equations proposed in reference 9, table II presents parameters necessary to calculate the mean-depth-of-erosion-versus-time curve for stainless steel, mild steel, and brass tested in a liquid impact device (ref. 26). In order to use this method, one must know the two steady-state periods. These may, however, not be available for most of the materials tested. The curve-fit approach suggested by this laboratory (ref. 14) produces a large scatter band to cover a wide variety of experimental conditions. This method, however, not only calculates erosion rates and times, but also the cumulative erosion.

In addition to a curve-fit approach (ref. 14) suggested earlier to solve long-term predictions, a new characteristic law of average erosion rate versus cumulative erosion is also presented herein.

Characteristic of Erosion-Rate-Versus-Cumulative-Erosion Curve

Figure 10 presents a typical plot of cumulative average volume loss rate versus volume loss of mild steel tested in a rotating disk device. The experimental conditions are: pressure, 0.15 MPa (abs); velocity, 37.3 m/sec; diameter of the cavitation inducer, 25.4 mm; and diameter of the test specimen, 63.5 mm. It appears that this curve has acceleration, peak rate, and decelera-

tion zones. The acceleration and deceleration zones may be represented by separate power-law relations. The equation for the acceleration zone is written as:

$$V/t = AV^n \quad (1)$$

or $$V = (At)^{1/(1-n)} \quad (2)$$

where V = cumulative volume loss, mm^3; t = exposure time corresponding to V, min; A = coefficient; and n = exponent. Differentiation of equation (2) with respect to t and after simplification results in

$$dV/dt = V/[(1-n)t] \quad (3)$$

Similarly, the deceleration zone after the peak is represented as

$$V/t = BV^{-m} \quad (4)$$

or $$V = (Bt)^{1/(1+m)} \quad (5)$$

where B = coefficient, and m = exponent. Differentiation of equation (5) with respect to t results in:

$$dV/dt = V/[(1+m)t] \quad (6)$$

$$= C\, t^{-p\,(1+m)} \quad (7)$$

where $C = B^{1/(1+m)}$ and $p = m/(1+m)$. The coefficients, exponents (slopes), and correlation coefficients obtained by least-square fit are marked on figure 10. Equation (3) and (6) indicate that instantaneous erosion rate dV/dt for these two zones is a function of cumulative average erosion rate V/t. Further the ratios of these two rates are always constant. The intersection point for these two curves may be obtained by equating equations (1) and (4), i.e.,

$$AV^n = BV^{-m} \quad (8)$$

or $$V = (B/A)^{1/(n+m)} \quad (9)$$

The value of V in equation (9) corresponds to maxima on average-erosion-rate-versus-erosion curve, and values of $(V/t)_{max}$ and time corresponding to this peak may be obtained by using either equation (1) or (4).

This study establishes that exponents n and m are almost equal, and that a power-law relation also exists between instantaneous erosion rate and exposure time. The advantage of this characteristic relation is that the values of $(dV/dt)_{max}$ and time corresponding to this peak may be calculated with only a few experimental points. It is generally observed that equation (1) terminates at $(dV/dt)_{max}$ and deviates from the experimental points. To the knowledge of the present authors this type of power-law relationship has not been reported earlier. This relationship opens new avenues in erosion scaling and modeling efforts.

CONCLUSIONS

A brief overview of long-term cavitation erosion prediction equations and their capabilities is presented. Data analysis using cavitation and liquid impingement erosion data indicates that the normalized curve-fit approach

suggested from this laboratory affords a better prediction for certain sets of data. For individual materials at one experimental condition, however, the methods proposed by Thiruvengadam and Heymann are good immediately following the peak erosion rate.

A unique power-law relationship between average erosion rate and cumulative erosion is presented. It is believed that this relationship can solve some long-term modeling problems.

REFERENCES

1. Honegger, E.: Tests on Erosion Caused by Jets. Brown Boveri Rev., vol. 14, no. 4, Apr. 1927, pp. 96-104.
2. Fyall, A. A.; King, R. B.; and Strain, R. N. C.: Rain Erosion - Part II and Part III. RAE-CHEM-510, RAE-CHEM-513, Royal Aircraft Establishment, 1957.
3. Hobb, J. M.: Cavitation Erosion Testing Techniques. NEL Rept. 69, National Engineering Laboratory, 1962.
4. Thiruvengadam, A.: Cavitation and Cavitation Damage. M. Sc. Thesis, Indian Institute of Science, 1959.
5. Thiruvengadam, A.: Prediction of Cavitation Damage. Ph. D. Thesis, Indian Institute of Science, 1961.
6. Thiruvengadam, A.; and Preiser, H. S.: On Testing Materials for Cavitation Damage Resistance. J. Ship Res., vol. 8, no. 3, Dec. 1964, pp. 39-56.
7. Plesset, M. S.; and Devine, R. E.: Effect of Exposure Time on Cavitation Damage. J. Basic Eng., vol. 99, no. 4, Dec. 1966, pp. 691-705.
8. Heymann, F. J.: On the Time Dependence of the Rate of Erosion due to Impingement or Cavitation. Erosion by Cavitation or Impingement, ASTM STP-408, American Society for Testing and Materials, 1967, pp. 70-110.
9. Tichler, J. W.; and de Gee, A. W. J.: Time Dependence of Cavitation Erosion and the Effect of Some Material Properties. Preceedings of the 3rd International Conference on Rain Erosion and Associated Phenomena, A. A. Fyall and R. B. King, eds., Royal Aircraft Establishment, 1970, pp. 847-879.
10. Thiruvengadam, A.: Theory of Erosion. Proceedings of the 2nd Meersburg Conference on Rain Erosion, A. A. Fyall and R. B. King, eds., Royal Aircraft Establishment, 1967, pp. 605-653.
11. Hoff, G.; and Langbein, G.: Resistance of Materials Towards Various Types of Mechanical Stress. Proceedings of the 2nd Meersburg Conference on Rain Erosion, A. A. Fyall and R. B. King, eds., Royal Aircraft Establishment, 1967, pp. 655-681.
12. Heymann, F. J.: Toward Quantitative Prediction of Liquid Impact Erosion. Characterization and Determination of Erosion Resistance, ASTM STP-474, American Society for Testing and Materials, 1970, pp. 212-248.
13. Noskievic, J.: Dynamics of the Cavitation Damage. Proceedings of the Joint IAHR/ASME/ASCE Symposium on Design and Operation of Fluid Machinery, vol. 2, Colorado State University, 1978, pp. 453-462.
14. Rao, P. V.; and Young, S. G.: Universal Approach to Analysis of Cavitation and Liquid-Impingement Erosion Data. NASA TP-2061, 1982.
15. Rao, P. V.; and Buckley, D. H.: Cavitation and Liquid Impingement Erosion Models for Long-Term Prediction - a Comparative Study.

16. Engel, O. G.: A First Approach to a Microscopic Model of Erosion Rate in Drop Impact and Cavitation. Proceedings of the 3rd International Conference on Rain Erosion and Associated Phenomena, A. A. Fyall and R. B. King, eds., Royal Aircraft Establishment, 1970, pp. 447-518.
17. Perelman, R. G.; and Denisov, Y. D.: The Strength of Materials Under the Action of Droplet Impacts. RAE Lib. Trans. No. 1654, 1971.
18. McGuiness, T.; and Thiruvengadam, A.: Cavitation Erosion - Corrosion Modeling. Erosion, Wear and Interfaces with Corrosion, A. Thiruvengadam, ed., ASTM STP-567, American Society for Testing and Materials, 1974, pp. 30-55.
19. Handbood of Cavitation Damage. TR-233-8, Hydronautics, Inc., 1965.
20. Lichtarowicz, A.: Cavitation Jet Apparatus for Cavitation Erosion Testing. Erosion: Prevention and Useful Application, W. F. Adler, ed., ASTM STP-664, American Society for Testing and Materials, 1979, pp. 530-549.
21. Thiruvengadam, A.: Handbook of Cavitation Erosion. TR-7301-1, Hydranautics, Inc., 1974.
22. Thiruvengadam, A.: On the Selection of Modelling Materials to Scale Long-Term Erosion of Prototype Systems. Proceedings of the 3rd International Conference on Rain Erosion and Associated Phenomena, A. A. Fyall and R. B. King, eds., Royal Aircraft Establishment, 1970, pp. 565-599.
23. Schmitt, G. F. Jr.: Liquid and Solid Particle Impact Erosion. Wear Control Handbook, M. P. Peterson and W. O. Winer, eds., American Society of Mechanical Engineers, 1980, pp. 231-282.
24. Kerr, S. L.: Determination of the Relative Resistance to Cavitation Erosion by the Vibratory Method. Trans. ASME, vol. 59, no. 5, July 1937, pp. 373-397.
25. Young, S. G.; and Johnston, J. R.: Effect of Temperature and Pressure on Cavitation Damage in Sodium. Characterization and Determination of Erosion Resistance, ASTM STP-474, American Society for Testing and Materials, 1970, pp. 67-108.
26. Thomas, G. P.; and Brunton, J. H.: Drop Impingement Erosion of Metals. Proc. Roy. Soc. Lordon, vol. 314A, Jan. 1970, pp. 549-565.
27. Elliott, D. E.; Marriott, J. B.; and Smith, A.: Comparison of Erosion Resistance of Standard Steam Turbine Blade and Shield Materials on Four Test Rigs. Characterization and Determination of Erosion Resistance, ASTM STP-474, American Society for Testing and Materials, 1970, pp. 127-161.

TABLE I. - PREDICTIVE MODELS, FORMULATIONS, AND PARAMETERS NECESSARY FOR COMPUTATION OF CAVITATION AND LIQUID-IMPINGEMENT EROSION VERSUS TIME CURVES

Investigator	Type of erosion[a]	Parameters needed for computation
Thiruvengadam (refs. 19 and 21)	CAV (nomogram)	(1) erosion intensity (2) strain energy
Heymann (ref. 8)	CAV and LI (elementary model)	(1) Nominal mean lifetime for original surface (2) Standard deviation for original surface (3) Nominal mean lifetime for substructure (4) Standard deviation for substructure
	LI (elaborated) model)	(1) Delay time during which no failure occurs (2) Mean of log-normal distribution on logarithmic time scale (3) Standard deviation of log-normal distribution on logarithmic time scale
Thiruvengadam (ref. 10)	LI and CAV	(1) Magnitude of instantaneous erosion rate at first peak, I_{max} (2) Time to attain first peak instantaneous erosion rate, t_m (3) Attenuation exponent, n (4) Weibull shape parameter, α
Hoff and Langbein (ref. 11)	LI (rain erosion)	(1) Maximum rate of erosion, e_{max} (20 Incubation period (intercept on time axis from straight line portion of erosion vs. time curve), t
Heymann (ref. 12)	CAV and LI	(1) Mean depth of erosion at tangent point, y_T (2) Average erosion rate at tangent point, R_T (3) Exponential constant, B
	LI	(1) Cumulative mean depth of erosion or material loss at tangent point, y_T (2) Normal component of impact velocity, V_o (3) Volume of liquid impinging per unit area per unit time, U_a (4) Generalized nondimensional erosion resistance parameter. N_e

Investigator	Type of erosion[a]	Parameters needed for computation
Tichler and de Gee (ref. 9)	CAV	(1) Incubation time, t_o (2) Resistance against cavitation erosion under hydrodynamic conditions, as occur in magnetostrictive oscillator R_c (3) Mean depth of erosion at which effect of crater formation becomes manifest, r_b (4) Proportionality constant, symbolizing increase in mean depth of erosion that would be necessary to form number of craters per unit area in final of craters per unit area in final steay-state period, κ (5) Ratio of rate of erosion in the final steady-state period to rate of erosion in first steady-state period, ϕ^∞
Perelman and Denisov (ref. 17)	LI	(1) work done on microplastic deformations per cycle of load, due to the energy capacity of microvolumes of the material (2) energy expended on fatigue fracture (3) influence of the surface form (4) kinetic energy of a stream of droplets (5) energy in a steam of droplets absorbed during the incubation period (6) specific energy of fracture determined from macroscopic fracture tests (7) energy absorbed by the material during initial deformation
Thiruvengadam (ref. 23)	CAV and LI (nomogram)	(1) erosion intensity (2) erosion strength
Lichtarowicz (ref. 20)	LI (graph)	(1) cumulative peak erosion rate (2) time to reach cumulative peak erosion rate
Noskievic (ref. 13)	CAV	(1) Cavitation property of material, β (2) Cavitation strength of material or inner friction of material during plastic deformation, α (3) Cavitation damage rate in developed period of cavitation attack, v_s
Rao and Young (ref. 14)	CAV and LI	(1) Peak cumulative average erosion rate (2) Time to attain peak cumulative average erosion rate (3) Incubation period (4) Erosion resistance

[a]CAV: cavitation erosion
LI: liquid impingement erosion, cylindrical/spherical drop or jet impact including jet with cavitation inducer.

TABLE II - PARAMETERS NECESSARY FOR TICHLER AND DE GEE MODEL
Data source: ref. 26

Parameter	Stainless Steel	Mild steel	60/40 brass
t_o, impacts	252×10^3	85×10^3	189×10^3
R_c	2.32×10^{-3}	2.72×10^{-3}	4.20×10^{-3}
r_b, μm	328	360	620
R_∞	5.19×10^{-4}	1.46×10^{-3}	3.44×10^{-4}
$\phi = R_\infty / R_c$	0.244	0.536	0.082
α	1.422	-----	0.763
β	1.813	-----	3.395
$r(t_s)$	369	401	722
r_s	392	453	849
κ	75.62	-----	-----

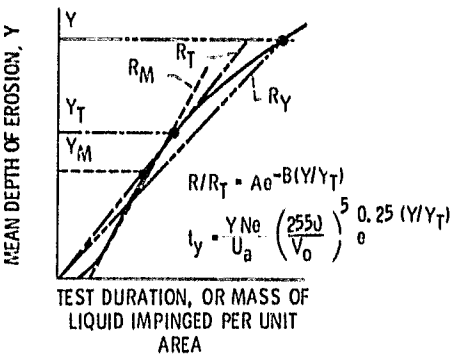

Figure 1. - Typical cumulative erosion versus time curve, defining various terms used and equations suggested. (Ref. 11).

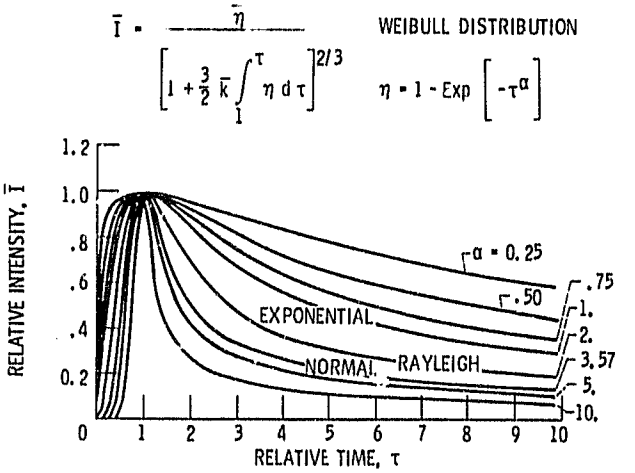

Figure 2. - Theoretical prediction of the effect of time on intensity of erosion when n = 2 (Ref. 9).

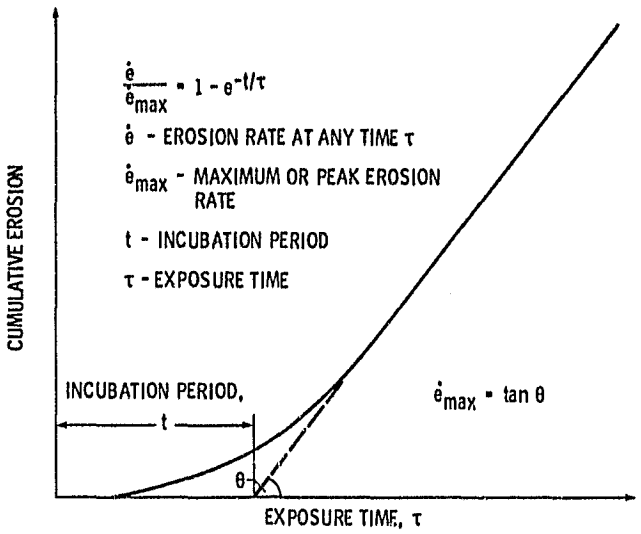

Figure 3. - Schematic of erosion versus time curve depicting incubation period according to Hoff & Langbein (ref. 10).

$$r = r_b + K \log\left[1 - \frac{1}{\varphi_\infty} + \frac{1}{\varphi_\infty} \exp \frac{\varphi_\infty (t - t_0 - R_c r_b)}{K R_c}\right]$$

$$K = \frac{r_s - r(t_s)}{\log\left[1 / \left\{1 - (1 - \varphi_\infty)\frac{\varphi_\infty}{1 - \varphi_\infty}\right\}\right]}$$

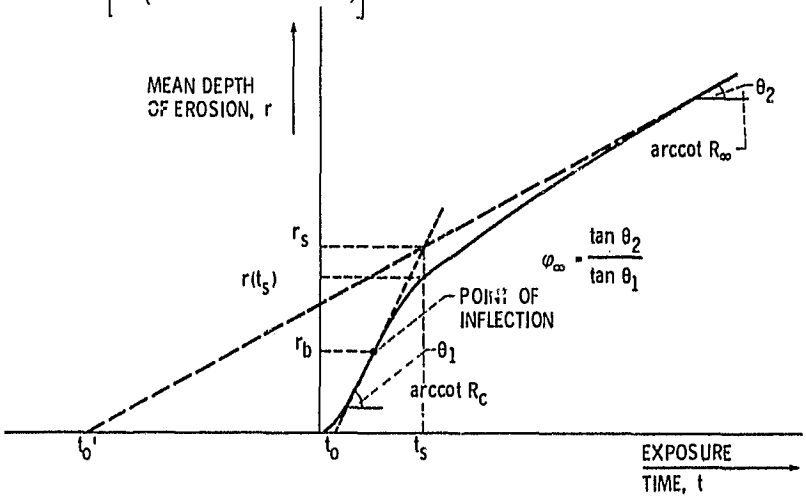

Figure 4. - Equation and definition of parameters used by Tichler and de Gee (ref. 8).

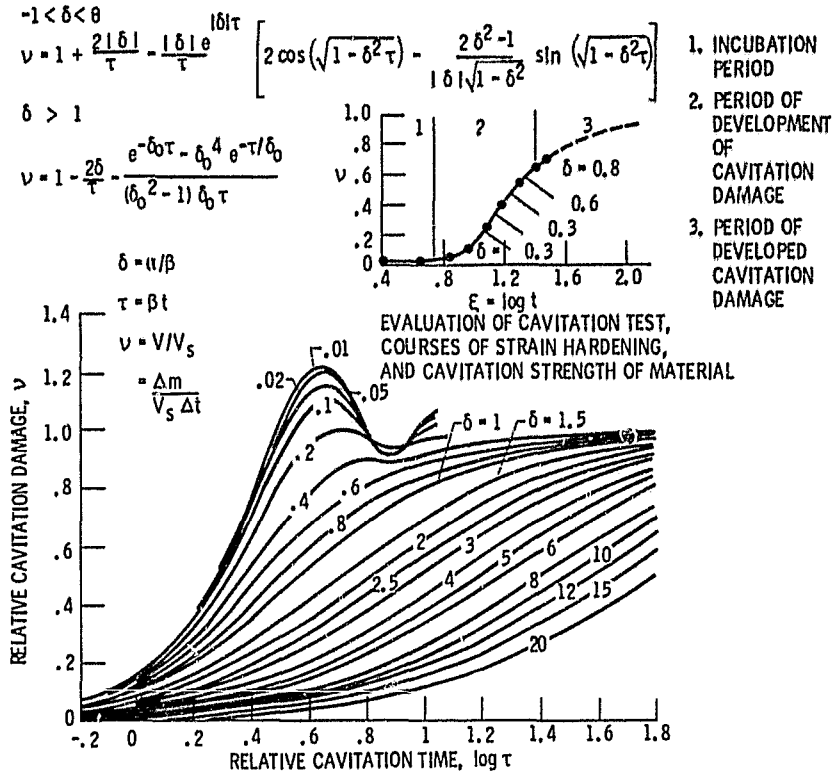

Figure 5. - Relative cavitation damage versus relative time curves (ref. 12).

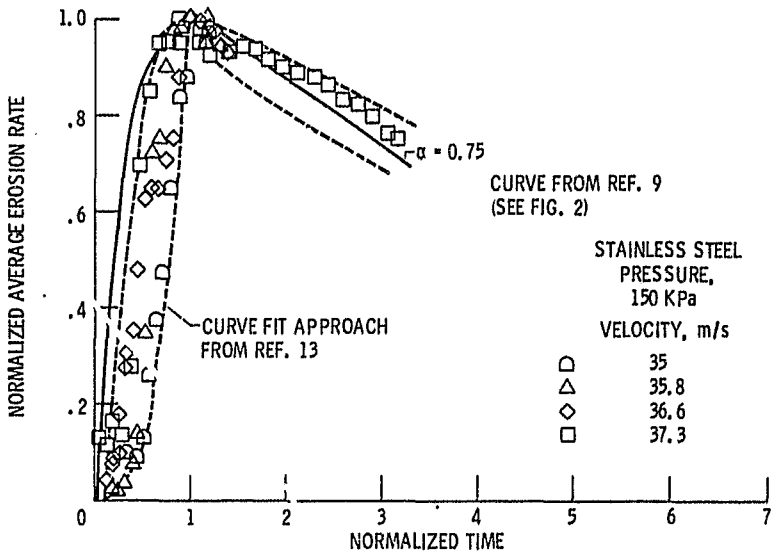

Figure 6. - Normalized average erosion rate versus normalized time of stainless steel in a rotating disk device.

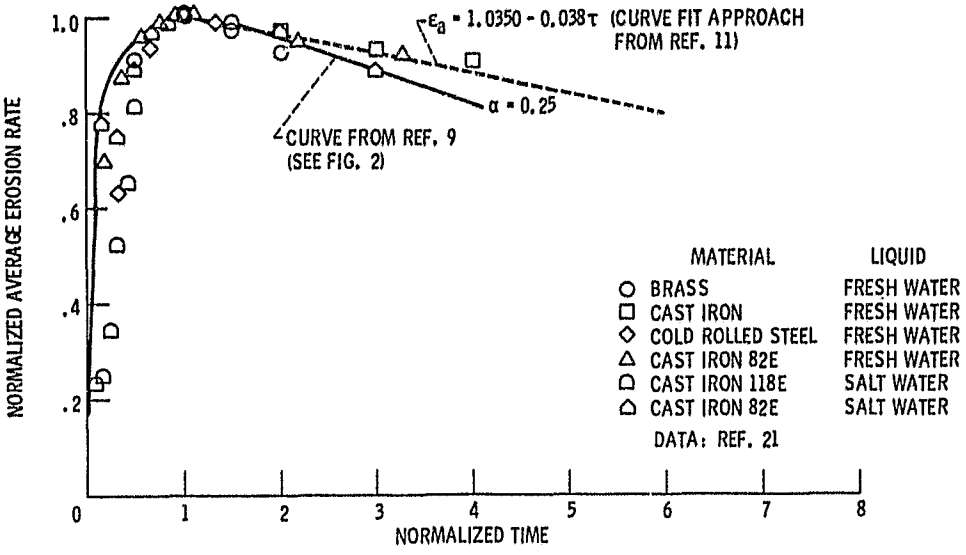

Figure 7. - Normalized average erosion rate versus normalized time of different materials - vibratory cavitation.

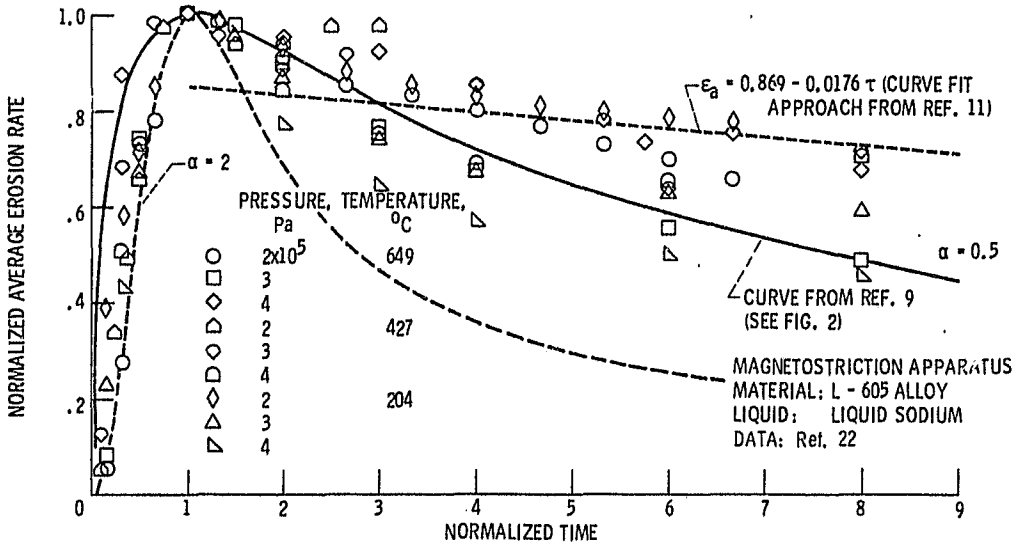

Figure 8. - Normalized average erosion rate versus normalized time of L-605 alloy tested at different temperatures in liquid sodium.

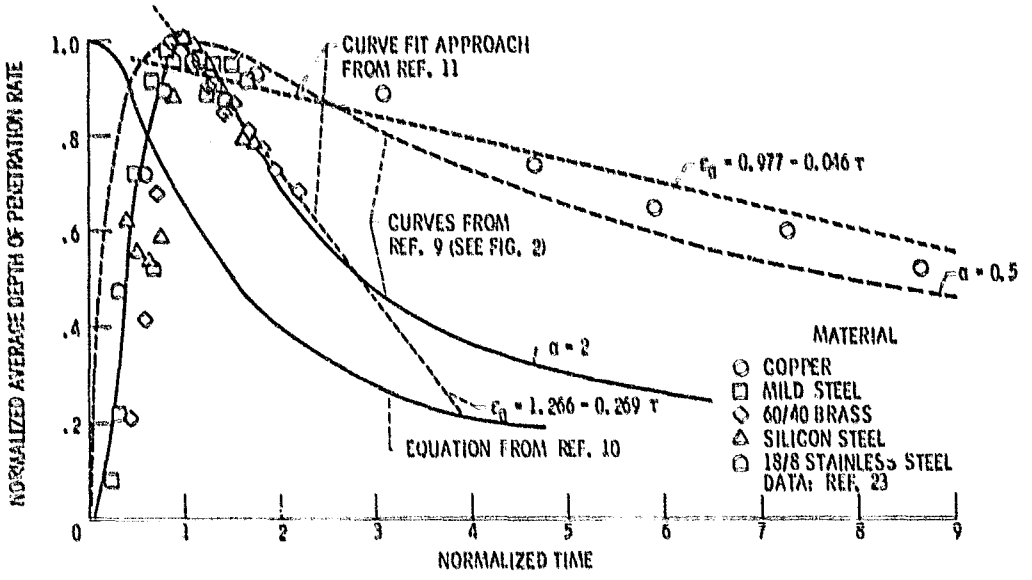

Figure 9. - Normalized average erosion rate versus normalized time for different materials - drop impingement.

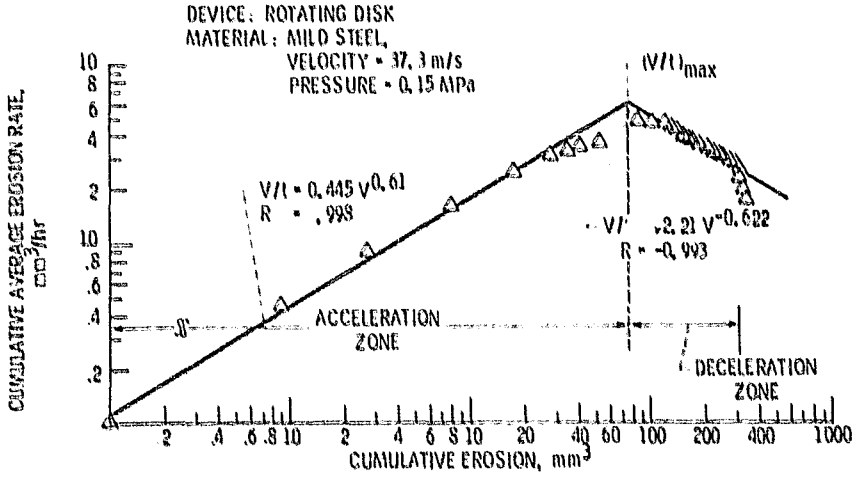

Figure 10. - Average erosion rate as function of cumulative erosion.